



PERGAMON

International Journal of Solids and Structures 38 (2001) 2597–2613

INTERNATIONAL JOURNAL OF
SOLIDS and
STRUCTURES

www.elsevier.com/locate/ijsolstr

Mode separation of energy release rate for delamination in composite laminates using sublaminates

Z. Zou, S.R. Reid, P.D. Soden, S. Li *

Department of Mechanical Engineering, UMIST, P.O. Box 88, Manchester M60 1QD, UK

Received 9 November 1999; in revised form 7 April 2000

Abstract

Individual energy release rates for delamination in composite laminates do not exist according to two- or three-dimensional elastic theory due to the oscillatory characteristics of the stress and displacement fields near the delamination tip (Sun, C.T., Jih, C.J., 1987. Engng. Fracture Mech. 28, 13–20; Raju, I.S., Creus Jr., J.H., Aminpour, M.A., 1988. Engng. Fracture Mech. 30, 383–396.) In this paper, sublaminates governed by transverse shear deformable laminate theory are adopted to model such delamination. Oscillatory singular stresses around the delamination tip are avoided as a result. Instead, stress resultant jumps are found in the sublaminates across the delamination tip. It transpires that mode I, II and III energy release rates can then be obtained using the virtual crack closure technique. The results produced by this approach for a homogeneous double cantilever beam and an edge-delamination in a non-homogeneous laminate show good agreement with those available in the literature. The approach produces both total and individual components of energy release rate for delamination, which converge as the sublamine division is refined and the sizes of the delamination tip elements decrease. © 2001 Elsevier Science Ltd. All rights reserved.

Keywords: Energy release rate; Delamination; Sublamine; VCCT; Laminated composites; Mixed mode fracture

1. Introduction

One of the most frequently encountered forms of damage in composite laminates is delamination, essentially interface cracks between the plies. Theoretical studies of the propagation of existing delaminations have to date been carried out mainly by adopting fracture mechanics to deal with the singularity at a delamination leading edge or tip. The propagation of an existing delamination is governed by the magnitudes of stress intensity factors or energy release rates. However, unlike cracks in homogeneous bodies, linear elastic fracture mechanics based upon a two- or three-dimensional theory has encountered considerable difficulties when dealing with these interfacial cracks which have not yet been overcome satisfactorily. The mismatch of material properties across the interface always results in coupled fracture modes.

*Corresponding author. Fax: +44-0161-200-3737.

E-mail address: shuguang.li@umist.ac.uk (S. Li).

The stress fields around the crack tip show an oscillatory singularity (Williams, 1959), as do the relative displacements between the surfaces of the crack (England, 1965). This leads to physically inadmissible interpenetration of crack surfaces near crack tips.

Several types of stress intensity factors have been introduced to characterise crack tip stress fields (Rice and Sih, 1965; Wang, 1983; Rice, 1988; Suo, 1990; Wu, 1990). However defined, for interfacial cracks in dissimilar media, these stress intensity factors do not carry the classical physical interpretations which identify three independent singular fields, referred to as the three modes of singularity, as in a homogeneous body. This leaves a gap which needs to be bridged before the theory can be applied to practical problems.

It has also been found that individual components of energy release rate for an interface crack expressed in terms of classical crack closure integrals or the virtual crack closure technique (VCCT) for solid finite element analysis are not well defined because they do not converge. Rather, they show oscillatory behaviour as do the stresses and displacements (Sun and Jih, 1987; Raju et al., 1988). Although the total energy release rate does converge to a definite value, using it as a criterion for delamination growth is limited when a mixed mode is involved (Hutchinson and Suo, 1992).

Some researchers (Hwu and Hu, 1992; Toya et al., 1997) modified the definition of energy release rates by using a finite crack extension, larger than the size of the oscillation region, instead of the infinitesimal one in the conventional definition. However, choosing the magnitude of the finite crack extension lacks sound theoretical or experimental grounds. Raju et al. (1988) modelled resin-rich layers of about 0.01 mm thickness between neighbouring plies as physical entities. A crack was assumed to exist centrally within this resin layer. As a result, the oscillation vanished. The numerical results showed that the individual components as well as the total energy release rates remain unchanged when the sizes of the crack tip elements decrease. Unfortunately, the resin-rich layer is too thin to be modelled in practical problems.

For delaminations in composite laminates, it is preferable to use laminate theory rather than three-dimensional elasticity theory. It is computationally expensive to use solid finite elements because a large number of elements through the laminate thickness are required, especially in the case of multiple delamination problems. Attempts to obtain individual fracture modes from laminate theory can be found in a number of publications. Williams (1988) suggested that mode I delamination be represented by a pair of moments and transverse shear forces acting in opposite directions applied to the opposite sides of the delamination. Mode II is obtained when the curvatures in the two parts of a delaminated laminate are the same. The underlying justification for this approach is associated with the relative displacements between the surfaces of the delamination around its tip. The opening displacement produces mode I while mode II corresponds to an in-plane sliding displacement. However, a pair of moments acting in opposite directions applied to a split beam with two arms of different thickness, for example, results in non-zero relative sliding displacement. This means that it is a mixed mode rather than a pure mode I problem (Suo and Hutchinson, 1990). With the help of a two-dimensional asymptotic numerical solution for a semi-infinite interface crack between two elastic layers given by Suo and Hutchinson (1990), Toya et al. (1997) calculated the energy release rates for mode I and mode II by a straightforward application of the crack closure method with finite crack extension. Strictly speaking, this approach is valid only for laminates consisting of only two different layers. This is far too restrictive to be applied to practical laminates. Sheinman and Kardomateas (1997) used the elastic property smearing technique to convert the problem of a delaminating beam into an equivalent homogeneous problem with orthotropic behaviour through the beam thickness and separated the individual modes. In such smearing techniques, the effects of ply stacking sequence are ignored completely. This may cause errors depending on the nature of the beam. When laminate theory is used and the laminate is considered to be comprised of two sublaminates in the delaminated region and a single intact laminate in the undelaminated region (the model adopted widely in the literature), the moments contributing to both mode I and mode II will inevitably be involved in the expression for total energy release rate. Individual components cannot be separated directly. Various assumptions have to be made to reach this goal which require justification.

Unlike the above laminate models, in this paper, the laminate is divided into sublaminates in both delaminated and undelaminated regions with transverse shear-deformable laminate theory being adopted for each of the sublaminates. The use of laminate theory eliminates the stress singularity and the oscillatory behaviour involved in two- or three-dimensional linear elastic fracture mechanics theory for this problem. Instead, stress resultants may show discontinuities across the delamination tip which reflects the interfacial stress singularity there. Since there are no interfacial moments between the sublaminates (as will be discussed later), individual components of energy release rate can be obtained using the VCCT. They are all well defined according to their classical definitions and converge to definite values as the magnitude of the virtual delamination extension reduces. This approach will be applied to standard delamination problems concerning a homogeneous double cantilever beam and a non-homogeneous edge delaminated composite laminate. The results show good agreement with those in the literature. As will be shown, usually more than two sublaminates through the laminate thickness are required even for single delaminations in order to reflect the three-dimensional nature of the problem with reasonable accuracy.

2. Sublamine theory

The laminates considered in this paper comprise unidirectional plies with arbitrary lay-up angles and are assumed to be delaminated prior to loading by a number of through-width delaminations located arbitrarily as shown in Fig. 1(a). Based on the configuration of the delaminated laminate, it is natural to

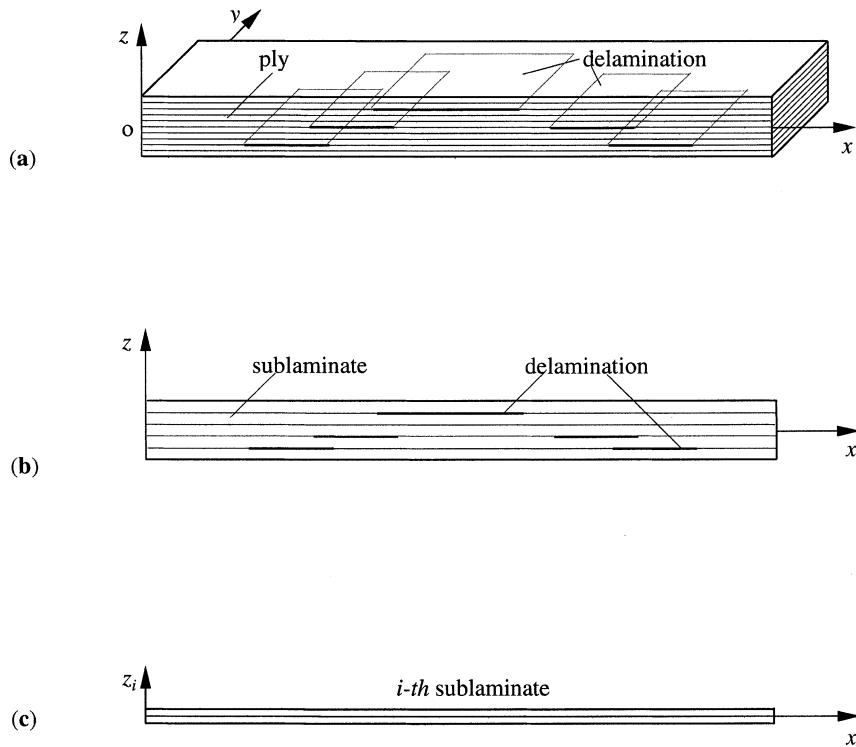


Fig. 1. Configuration of the delaminated laminate: (a) plies and delaminations, (b) sublaminates and delamination and (c) local coordinate of sublamine.

consider the delaminated laminate as an assembly of sublaminates each of which may consist of several plies or parts of plies through the laminate thickness so that the delaminations exist at the interfaces of the sublaminates, as shown in Fig. 1(b).

In the present work, the laminate is assumed to be subjected to loads which are constant in the width, i.e. y direction. The problem considered is essentially two-dimensional. The width of the laminate is large relative to the dimension of the zone affected by the crack tip. Thus, the problem can be presented as a generalised plane strain problem in which all the strain components of the laminate are independent of the coordinate y . For each sublamine, its mid-surface is taken to be the reference surface, as shown in Fig. 1(c). According to the first order transverse shear deformable laminate theory (Reissner, 1945), the displacements in the i th sublamine can be expressed as

$$\begin{aligned}\tilde{u}_i(x, y, z_i) &= u_i(x) + z_i \alpha_i(x) - \varepsilon_1 y^2 / 2, \\ \tilde{v}_i(x, y, z_i) &= v_i(x) - z_i \beta_i(x) + \varepsilon_0 y + \varepsilon_1 x y + \kappa_0 y (z_i + h_i), \\ \tilde{w}_i(x, y, z_i) &= w_i(x) - \kappa_0 y^2 / 2,\end{aligned}\quad (1)$$

where u_i , v_i and w_i are the displacements at its mid-plane and α_i and β_i , the rotations of the normals of sublamine about the y and x axes. z_i is the local coordinate for the sublamine in the thickness direction. h_i is the global z -coordinate of the mid-plane of the i th sublamine. ε_0 , ε_1 and κ_0 are given constants for the whole laminate which are associated with the generalised strains in a generalised plane strain problem in the $x-z$ plane as shown in Fig. 1.

The generalised strains in the i th sublamine are

$$\begin{aligned}\varepsilon_{xi}^0 &= u'_i, \quad \kappa_{xi} = \alpha'_i, \\ \varepsilon_{yi}^0 &= \varepsilon_0 + \varepsilon_1 x + \kappa_0 h_i, \quad \kappa_{yi} = \kappa_0, \\ \gamma_{xyi}^0 &= v'_i, \quad \kappa_{xyi} = -\beta'_i, \\ \gamma_{xzi} &= w'_i + \alpha_i, \quad \gamma_{yzi} = -\beta_i,\end{aligned}\quad (2)$$

where the prime denotes the derivative with respect to x .

The interfacial displacement continuity conditions between any two neighbouring sublaminates, e.g. the i th and $(i+1)$ th sublaminates, in the undelaminated region are

$$\begin{aligned}u_i + t_i \alpha_i / 2 &= u_{i+1} - t_{i+1} \alpha_{i+1} / 2, \\ v_i - t_i \beta_i / 2 &= v_{i+1} + t_{i+1} \beta_{i+1} / 2, \\ w_i &= w_{i+1},\end{aligned}\quad (3)$$

where t_i and t_{i+1} are the thicknesses of the i th and $(i+1)$ th sublaminates, respectively.

3. The virtual crack closure technique

A solid finite element mesh around a crack tip is shown in Fig. 2. The physical interpretation of VCCT is that the energy released during the virtual crack extension by a length of Δa is equal to the work required to close the crack to its original length while the external loading remains unchanged. In a finite element representation, the energy released is half of the work done by the forces at nodes c and d required to pull them together; therefore, (Rybicki and Kanninen, 1977)

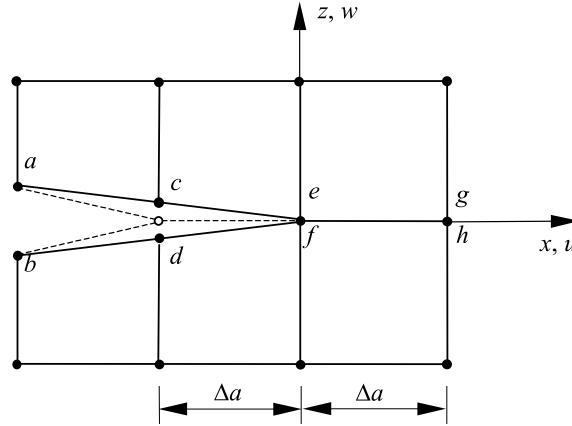


Fig. 2. Solid finite element mesh around the crack tip.

$$\begin{aligned}
 G_I &= \frac{1}{2\Delta a} Z_{cd}(w_c - w_d), \\
 G_{II} &= \frac{1}{2\Delta a} X_{cd}(u_c - u_d), \\
 G_{III} &= \frac{1}{2\Delta a} Y_{cd}(v_c - v_d),
 \end{aligned} \tag{4}$$

$$\text{and } G = G_I + G_{II} + G_{III}, \tag{5}$$

where G_I , G_{II} and G_{III} are the energy release rate for modes I to III and G is the total energy release rate. X_{cd} , Y_{cd} and Z_{cd} are the magnitudes of nodal force pairs at nodes c and d in the x , y and z directions, respectively, which are required to pull nodes c and d together. u_c , v_c , w_c and u_d , v_d , w_d are nodal displacements before nodes c and d are pulled together. Two separate analyses of two consecutive configurations are required to obtain the nodal forces and relative displacements.

When the above formulations are applied to delaminations in composite laminates, the individual energy release rates do not converge, but show oscillatory behaviour as Δa decreases (Sun and Jih, 1987; Raju et al., 1988) with physically inadmissible interpenetration of crack surfaces near crack tips. Solid finite elements also meet other difficulties in modelling composite laminates, especially delaminated laminates. If one ply is modelled by one or more layers of elements, the number of elements for the whole laminate could be enormous, especially for a thick laminate, in order to keep a reasonable element aspect ratio. When multiple delaminations are involved, this can easily make the problem computationally very expensive. If one includes several plies of different fibre orientations in one layer of elements, a stiffness smearing technique is normally used and the effects of stacking sequence cannot then be taken into account properly.

A laminate finite element mesh around a delamination tip is sketched in Fig. 3. To be consistent with the solid finite element method, the nodes are first placed at the delamination plane, i.e. lower and upper surfaces of the upper and lower sublaminates, respectively, as shown in Fig. 3(a).

In laminate theory, each node represents the whole cross-section of the sublamine; therefore, there are three displacements and two rotations of the cross-section at each node which are conjugate to three nodal forces and two nodal moments in the laminate finite elements. During the closing of a crack, the nodal moments, as well as the nodal forces, do work. From the physical interpretation of VCCT, the total energy release rate is

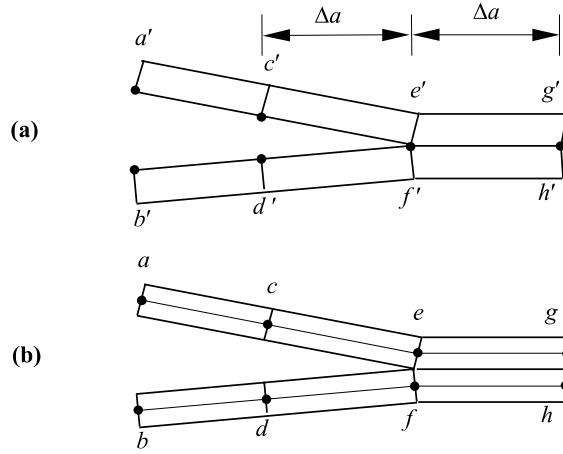


Fig. 3. Sublamine finite element mesh around the delamination tip.

$$G = \frac{1}{2\Delta a} \left\{ X_{c'd'}(u_{c'} - u_{d'}) + Y_{c'd'}(v_{c'} - v_{d'}) + Z_{c'd'}(w_{c'} - w_{d'}) + M_{c'd'}^y(\alpha_{c'} - \alpha_{d'} - \alpha_{c'}^0 + \alpha_{d'}^0) + M_{c'd'}^x(\beta_{c'} - \beta_{d'} - \beta_{c'}^0 + \beta_{d'}^0) \right\}, \quad (6)$$

where $u_{c'}$, $v_{c'}$, $w_{c'}$, $\alpha_{c'}$, $\beta_{c'}$ and $u_{d'}$, $v_{d'}$, $w_{d'}$, $\alpha_{d'}$, $\beta_{d'}$ are the generalised displacement components at nodes c' and d' . $\alpha_{c'}^0$, $\beta_{c'}^0$, $\alpha_{d'}^0$ and $\beta_{d'}^0$ are the rotations after the nodes c' and d' are closed. $X_{c'd'}$, $Y_{c'd'}$, $Z_{c'd'}$ and $M_{c'd'}^y$, $M_{c'd'}^x$ are the magnitudes of nodal forces and moments required to pull nodes c' and d' together.

It is clear that the three terms involving nodal forces contribute to the three modes, respectively. However, the last two terms involving nodal moments in Eq. (6) may contribute to all the modes unless the nodal moments are zero. In the laminate models adopted widely (Williams, 1988; Sheinman and Kardomateas, 1997; Toya et al., 1997), the undelaminated region is modelled as a single laminate. In this case, non-zero nodal moments are, in general, required to close nodes c' and d' . For example, consider a homogeneous double cantilever beam in Fig. 4. Only a nodal moment $M_{c'd'}^y$ of magnitude M is needed since the undelaminated region is modelled as a single laminate in which there will be no deformation under the given loading condition. The other nodal forces $X_{c'd'}$, $Y_{c'd'}$, $Z_{c'd'}$ and moment $M_{c'd'}^x$ are all zero. According to Williams (1988) intention, this is a pure mode I problem. However, two-dimensional analysis (Suo and Hutchinson, 1990) showed that this is a mixed-mode problem if the thicknesses of the two arms are different and the ratio of mode II to mode I varies when the depth of the delamination changes. It is impossible to

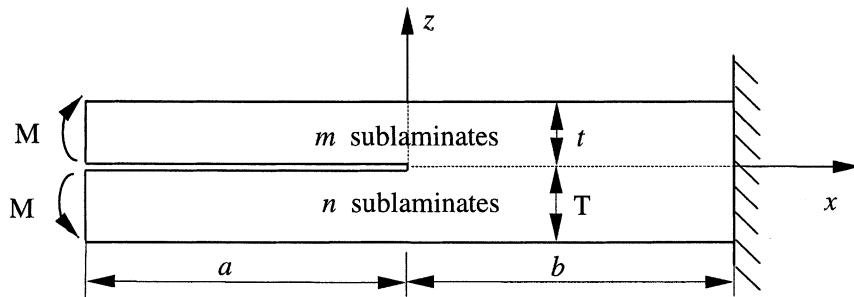


Fig. 4. Double cantilever beam under end moments.

separate the total energy release rate into individual components, in general, based on such a laminate model.

However, if the undelaminated region is also divided into sublaminates with independent rotations, governed by shear deformable laminate theory, individual energy release rates can then be obtained by VCCT since the nodal moments in Eq. (6) are always zero as will be discussed in the next two sections. With the dimension in the thickness direction eliminated in a laminate theory, there is no mechanism to accommodate stress singularity around the delamination tip and consequently, the oscillatory behaviour is not present. Instead, there exist stress resultant discontinuities across the delamination tip reflecting the effects of the singularity.

4. Interfacial forces

Of particular interest are the regions around the delamination tip in Fig. 1; therefore, for simplicity at this stage, only the part of the laminate behind and ahead of one delamination front is considered and two sublaminates are adopted, as shown in Fig. 5. It is assumed that the external forces only act on the two ends of the sublamine. With a variation of generalised displacements in the sublaminates, the corresponding variation of the total potential energy of the laminate under generalised plane strain conditions can be expressed as follows

$$\begin{aligned}
 \delta\Pi = & \int_0^l \sum_{i=1}^2 \left(N_{xi} \delta \dot{e}_{xi}^0 + N_{xyi} \delta \dot{\gamma}_{xyi}^0 + M_{xi} \delta \kappa_{xi} + M_{xyi} \delta \kappa_{xyi} + Q_{xi} \delta \gamma_{xzi} + Q_{yi} \delta \gamma_{yzi} \right) dx + \sum_{i=1}^2 \delta W_i \\
 = & - \sum_{i=1}^2 \int_0^a \left[N'_{xi} \delta u_i + N'_{xyi} \delta v_i + Q'_{xi} \delta w_i + (M'_{xi} - Q_{xi}) \delta \alpha_i - (M'_{xyi} - Q_{yi}) \delta \beta_i \right] dx \\
 & - \int_a^l \sum_{i=1}^2 \left[N'_{xi} \delta u_i + N'_{xyi} \delta v_i + Q'_{xi} \delta w_i + (M'_{xi} - Q_{xi}) \delta \alpha_i - (M'_{xyi} - Q_{yi}) \delta \beta_i \right] dx \\
 & + \sum_{i=1}^2 \left(N_{xi}^- \delta u_i^- + N_{xyi}^- \delta v_i^- + Q_{xi}^- \delta w_i^- + M_{xi}^- \delta \alpha_i^- - M_{xyi}^- \delta \beta_i^- \right) \\
 & - \sum_{i=1}^2 \left(N_{xi}^+ \delta u_i^+ + N_{xyi}^+ \delta v_i^+ + Q_{xi}^+ \delta w_i^+ + M_{xi}^+ \delta \alpha_i^+ - M_{xyi}^+ \delta \beta_i^+ \right) + \sum_{i=1}^2 (\delta \bar{W}_i + \delta W_i), \tag{7}
 \end{aligned}$$

where N_{xi} , N_{xyi} , Q_{xi} , Q_{yi} and M_{xi} , M_{xyi} are the stress resultants and moments, $\delta \bar{W}_i$ and δW_i , the variations of the potential energy of the internal and external forces at the two ends of the sublamine, respectively,

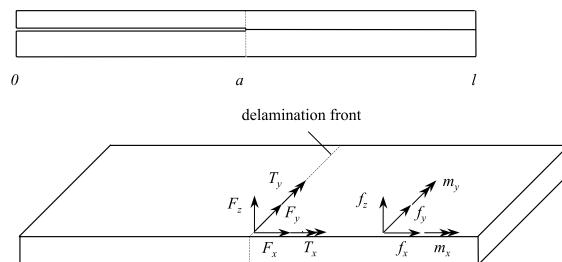


Fig. 5. Two sublaminated model and interfacial forces and moments.

which result in the natural boundary conditions. Superscript – or + indicates that the variable is evaluated at the delamination tip $x = a^-$ (in the delaminated region) or $x = a^+$ (in the undelaminated region), respectively.

For each sublamine, the generalised displacements are continuous across the delamination tip, i.e.,

$$[u_i^-, v_i^-, w_i^-, \alpha_i^-, \beta_i^-] = [u_i^+, v_i^+, w_i^+, \alpha_i^+, \beta_i^+] \quad (i = 1, 2). \quad (8)$$

In the undelaminated region $[a < x < l]$, the generalised displacements of the two sublaminates are dependent on each other, as expressed in Eq. (3). Using these relations, the three translational displacements at the mid-surface of the upper sublamine can be expressed in terms of the rest of the generalised displacements as follows:

$$\begin{aligned} u_2 &= u_1 + (t_1 \alpha_1 + t_2 \alpha_2)/2, \\ v_2 &= v_1 - (t_1 \beta_1 + t_2 \beta_2)/2, \\ w_2 &= w_1. \end{aligned} \quad (9)$$

Substituting Eqs. (8) and (9) into Eq. (7), these three generalised displacements can be eliminated and one obtains

$$\begin{aligned} \delta \Pi = - \sum_{i=1}^2 \int_0^a & \left[N'_{xi} \delta u_i + N'_{xyi} \delta v_i + Q'_{xi} \delta w_i + (M'_{xi} - Q_{xi}) \delta \alpha_i - (M'_{xyi} - Q_{yi}) \delta \beta_i \right] dx \\ & - \int_a^l \left[(N'_{x1} + N'_{x2}) \delta u_1 + (N'_{xy1} + N'_{xy2}) \delta v_1 + (Q'_{x1} + Q'_{x2}) \delta w_1 + (M'_{x1} - Q_{x1} + N'_{x2} t_1/2) \delta \alpha_1 \right. \\ & \quad \left. - (M'_{xy1} - Q_{y1} + N'_{xy2} t_1/2) \delta \beta_1 + (M'_{x2} - Q_{x2} + N'_{x2} t_2/2) \delta \alpha_2 - (M'_{xy2} - Q_{y2} + N'_{xy2} t_2/2) \delta \beta_2 \right] dx \\ & + (N_{x1}^- + N_{x2}^- - N_{x1}^+ - N_{x2}^+) \delta u_1^+ + (N_{xy1}^- + N_{xy2}^- - N_{xy1}^+ - N_{xy2}^+) \delta v_1^+ + [M_{x1}^- - M_{x1}^+ + (N_{x2}^- - N_{x2}^+) t_1/2] \delta \alpha_1^+ \\ & - [M_{xy1}^- - M_{xy1}^+ + (N_{xy2}^- - N_{xy2}^+) t_1/2] \delta \beta_1^+ + [M_{x2}^- - M_{x2}^+ + (N_{x2}^- - N_{x2}^+) t_2/2] \delta \alpha_2^+ \\ & - [M_{xy2}^- - M_{xy2}^+ + (N_{xy2}^- - N_{xy2}^+) t_2/2] \delta \beta_2^+ + (Q_{x1}^- + Q_{x2}^- - Q_{x1}^+ - Q_{x2}^+) \delta w_1^+ + \sum_{i=1}^2 (\delta \bar{W}_i + \delta W_i). \end{aligned} \quad (10)$$

According to the principle of minimum potential energy, the equilibrium conditions result in the generalised force continuity conditions at the delamination tip,

$$\begin{aligned} N_{x1}^- + N_{x2}^- &= N_{x1}^+ + N_{x2}^+, \\ N_{xy1}^- + N_{xy2}^- &= N_{xy1}^+ + N_{xy2}^+, \\ Q_{x1}^- + Q_{x2}^- &= Q_{x1}^+ + Q_{x2}^+, \\ M_{x1}^- - t_1 N_{x1}^-/2 &= M_{x1}^+ - t_1 N_{x1}^+/2, \\ M_{xy1}^- - t_1 N_{xy1}^-/2 &= M_{xy1}^+ - t_1 N_{xy1}^+/2, \\ M_{x2}^- + t_2 N_{x2}^-/2 &= M_{x2}^+ + t_2 N_{x2}^+/2, \\ M_{xy2}^- + t_2 N_{xy2}^-/2 &= M_{xy2}^+ + t_2 N_{xy2}^+/2, \end{aligned} \quad (11)$$

and the equilibrium equations of the laminate in the undelaminated region,

$$\begin{aligned}
N'_{x1} + N'_{x2} &= 0, \\
N'_{xy1} + N'_{xy2} &= 0, \\
Q'_{x1} + Q'_{x2} &= 0, \\
M'_{x1} - Q_{x1} - t_1 N'_{x1}/2 &= 0, \\
M'_{xy1} - Q_{y1} - t_1 N'_{xy1}/2 &= 0, \\
M'_{x2} - Q_{x2} + t_2 N'_{x2}/2 &= 0, \\
M'_{xy2} - Q_{y2} + t_2 N'_{xy2}/2 &= 0.
\end{aligned} \tag{12}$$

To obtain the individual modes of delamination, it is necessary to analyse the actions and reactions between the sublaminates, i.e. the interfacial forces at the delamination extension plane in the undelaminated region. At the junction, i.e., delamination tip, there may be, in general, concentrated interfacial forces F_x, F_y, F_z and moments T_x, T_y . Consider the lower sublaminates as a free body, as shown in Fig. 5. The equilibrium of an infinitesimal segment containing the delamination tip gives these concentrated forces and moments as

$$\begin{aligned}
F_x &= N_{x1}^- - N_{x1}^+, \\
F_y &= N_{xy1}^- - N_{xy1}^+, \\
F_z &= Q_{x1}^- - Q_{x1}^+, \\
T_y &= (M_{x1}^- - t_1 N_{x1}^-/2) - (M_{x1}^+ - t_1 N_{x1}^+/2), \\
T_x &= -\left(M_{xy1}^- - t_1 N_{xy1}^-/2\right) + \left(M_{xy1}^+ - t_1 N_{xy1}^+/2\right).
\end{aligned} \tag{13}$$

The distributed interfacial forces and moments acting on its top surface in the undelaminated region are f_x, f_y, f_z and m_x, m_y and can be obtained in a similar manner:

$$\begin{aligned}
f_x &= -N'_{x1}, \\
f_y &= -N'_{xy1}, \\
f_z &= -Q'_{x1}, \\
m_y &= -(M'_{x1} - Q_{x1} - t_1 N'_{x1}/2), \\
m_x &= M'_{xy1} - Q_{y1} - t_1 N'_{xy1}/2.
\end{aligned} \tag{14}$$

Comparing Eqs. (13) and (14) with Eqs. (11) and (12), it is concluded that

$$T_x = 0, \quad T_y = 0, \quad m_x = 0, \quad m_y = 0. \tag{15}$$

This same conclusion can also be obtained by considering the upper sublaminates as a free body. The first three equations in Eq. (14) show that the interfacial tractions can be expressed in terms of the derivatives of the stress resultants. The traction continuity conditions can be readily seen from the first three equations of Eq. (12) as a natural consequence of minimization of total potential energy.

The interfacial forces result from the constraints of displacement continuity, i.e. Eq. (3), between neighbouring sublaminates as reactions to the constraints. The relative rotations between sublaminates are free from any constraints and the zero interfacial moment conditions as given in Eq. (15) reflect this precisely. As a natural inference, the same conditions as expressed in Eq. (15) can be deduced for any inter-sublaminar interfaces when the laminate is modelled with more than two sublaminates. The concentrated and distributed interfacial forces for the delamination between i th and $(i+1)$ th sublaminates are

$$\begin{aligned}
F_x &= \sum_{j=1}^i (N_{xj}^- - N_{xj}^+), \quad f_x = -\sum_{j=1}^i N'_{xj}, \\
F_y &= \sum_{j=1}^i (N_{xyj}^- - N_{xyj}^+), \quad f_y = -\sum_{j=1}^i N'_{xyj}, \\
F_z &= \sum_{j=1}^i (Q_{xj}^- - Q_{xj}^+), \quad f_z = -\sum_{j=1}^i Q'_{xj}.
\end{aligned} \tag{16}$$

The absence of interfacial moments is a crucial step leading to the separation of individual modes. Eqs. (13)–(15) mean that the interfacial actions and reactions ahead of the delamination tip are the only three types of forces acting on the interface, the same as in the classical elasticity theory. These interfacial forces correspond to the three modes of fracture, respectively, according to fracture mechanics and the individual modes can be calculated by VCCT clearly in the context of laminate theory.

In previous laminate models (Williams, 1988; Sheinman and Kardomateas, 1997; Toya et al., 1997), the undelaminated region is modelled as a single laminate, which means that the rotations of all the sublaminates in the present model are the same. In this case, the continuity of moments across the delamination tip and moment equilibrium equations in the undelaminated region are

$$\begin{aligned}
M'_{x1} + M'_{x2} - Q_{x1} - Q_{x2} - (N'_{x1}t_1 - N'_{x2}t_2)/2 &= 0, \\
M'_{xy1} + M'_{xy2} - Q_{y1} - Q_{y2} - (N'_{xy1}t_1 - N'_{xy2}t_2)/2 &= 0, \\
M_{x1}^- + M_{x2}^- - (t_1 N_{x1}^- - t_2 N_{x2}^-)/2 &= M_{x1}^+ + M_{x2}^+ - (t_1 N_{x1}^+ - t_2 N_{x2}^+)/2, \\
M_{xy1}^- + M_{xy2}^- - (t_1 N_{xy1}^- - t_2 N_{xy2}^-)/2 &= M_{xy1}^+ + M_{xy2}^+ - (t_1 N_{xy1}^+ - t_2 N_{xy2}^+)/2.
\end{aligned} \tag{17}$$

From such a model, the interfacial moments, expressed in Eqs. (13) and (14), have to be present at the delamination tip and in the undelaminated region to maintain equilibrium and the total energy release rate cannot be separated into individual components in general.

5. Individual energy release rates

The nodal forces and moments required to close the nodes c' and d' are actually the effects of the interfacial concentrated and distributed forces and moments. Since there are no interfacial moments in the present laminate model, nodal moments must be zero. There are only three types of nodal forces, the same as in the solid finite element method. From Eqs. (4) and (6), the individual energy release rates are

$$\begin{aligned}
G_I &= \frac{1}{2\Delta a} Z_{c'd'}(w_{c'} - w_{d'}), \\
G_{II} &= \frac{1}{2\Delta a} X_{c'd'}(u_{c'} - u_{d'}), \\
G_{III} &= \frac{1}{2\Delta a} Y_{c'd'}(v_{c'} - v_{d'}).
\end{aligned} \tag{18}$$

When the size Δa of the delamination tip elements tends to zero, nodal forces $X_{c'd'}$, $Y_{c'd'}$ and $Z_{c'd'}$ at the delamination tip will be equal to the finite and determinate values of the stress resultant jumps F_x , F_y and F_z across the delamination tip as indicated in Eq. (16). Therefore, the energy release rate and its individual components tend to their limits as the size Δa of the delamination tip elements are made small enough.

In a laminate finite element representation, reference surfaces of the sublaminates and consequently, the nodes are usually placed at the mid-surfaces of the sublaminates as shown in Fig. 3(b), the interfacial forces or nodal forces are transferred to the mid-surface using the conditions of static equivalence. Therefore, the values of these forces remain the same and the nodal displacements at the delamination surfaces can be expressed in terms of the nodal displacements at the mid-surface of the sublaminates and rotations of the cross-sections. From Eqs. (3) and (18), the individual energy release rates for the delamination between the i th and $(i+1)$ th sublaminates can be expressed as follows:

$$\begin{aligned} G_I &= \frac{1}{2\Delta a} Z_{ef}(w_c - w_d), \\ G_{II} &= \frac{1}{2\Delta a} X_{ef}(u_c - u_d - t_{i+1}\alpha_c/2 - t_i\alpha_d/2), \\ G_{III} &= \frac{1}{2\Delta a} Y_{ef}(v_c - v_d + t_{i+1}\beta_c/2 + t_i\beta_d/2), \end{aligned} \quad (19)$$

where X_{ef} , Y_{ef} and Z_{ef} are the magnitudes of interacting nodal forces between nodes e and f which are approximations to the forces required to pull nodes c and d together when Δa is very small (Rybicki and Kanninen, 1977) and the same element size ahead of and behind node $e-f$ is maintained. In this way, the energy release rates are evaluated only from the results of a single analysis for one configuration.

The interfacial displacement continuity conditions, Eq. (3), can be included in a finite element model in different ways. In the present analysis, the commercial finite element package ABAQUS (HKS, 1996) was chosen as the solver. The option EQUATION was used to impose the continuity conditions. As for nodes e and f at the delamination tip, the displacement continuity conditions can be rewritten as

$$\begin{aligned} u_e - u_f - t_{i+1}\alpha_e/2 - t_i\alpha_f/2 - u_0 &= 0, \\ \phi v_e - v_f + t_{i+1}\beta_e/2 + t_i\beta_f/2 - v_0 &= 0, \\ w_e - w_f - w_0 &= 0, \end{aligned} \quad (20)$$

where u_0 , v_0 , and w_0 are displacement components of an extra node introduced artificially so that the nodal forces X_{ef} , Y_{ef} and Z_{ef} between node e and f can be obtained as the reactions at this node when it is fixed.

Having employed a laminate theory for the sublaminates, a smearing process can be used to evaluate the stiffnesses. This differs from the homogenisation process in the solid finite element approach as sublaminates here still preserve at least a first order level of heterogeneity represented by the constituent terms in their stiffness matrices [A], [B] and [D].

6. Effects of number of sublaminates on energy release rates

Individual fracture modes are classified with respect to the local symmetry conditions about the crack surface around the crack tip in fracture mechanics (Anderson, 1995). When a delaminated laminate is symmetric about the delamination plane, the two-sublaminates model can give reasonable results irrespective of the number of sublaminates introduced in the parts of the laminate on both side of the delamination, because the loading can always be separated into a symmetric part and an antisymmetric part and laminate theory produces symmetric and antisymmetric (in-plane and anti-plane) results which produce mode I, mode II and mode III, respectively. In general, such symmetry does not always exist in a delaminated laminate and the local deformation around the delamination tip may not be represented accurately by a laminate theory with a single sublamine on each side of the delamination. More sublaminates must be used to allow a reasonable distribution of the in-plane displacements over the laminate

thickness reflecting the two- or three-dimensional characteristics. The individual energy release rates are found to converge to their true values as the number of sublaminates increases.

Consider a double cantilever beam (DCB) as shown in Fig. 4. When it is considered as a semi-infinite split beam, a two-dimensional analytical solution has been given by Suo and Hutchinson (1990). This is reasonable when thicknesses t and T are much smaller than lengths a and b . The material is homogeneous and isotropic and, therefore, it is a conventional elastic fracture mechanics problem without oscillatory behaviour.

The total energy release rate can be expressed as (Suo and Hutchinson, 1990)

$$G_t = \frac{6M^2}{E} \left(\frac{1}{t^3} + \frac{1}{T^3} \right), \quad (21)$$

where E is Young's modulus of the material. The classical mode I and II stress intensity factors, K_I and K_{II} are obtained from an asymptotic numerical analysis in their paper.

In order to compare the present approach with the two-dimensional analytical results of Suo and Hutchinson (1990), the following relationship between stress intensity factors and energy release rates is used (Rybicki and Kanninen, 1977)

$$K_{II}/K_I = \sqrt{G_{II}/G_I}. \quad (22)$$

Consider first the DCB to comprise two sublaminates, above and below the delamination. The numerical results are given in Table 1. Although the total energy release rate agrees well with Eq. (21), the individual components drift away as the ratio of the two thicknesses decreases from unity.

However, if the two sublaminates are further divided uniformly into m and n sublaminates, respectively, the results improve rapidly as m and n increase and approach the two-dimensional solution, as shown in Table 2. A range of thickness ratios has been analysed and the results are shown in Table 3. It can be seen that even when the delamination is near one of the beam's surfaces, $t/T = 0.2$, the number of sublaminates required to achieve a reasonable approximation is acceptable.

Table 1
Results for different thickness ratios of a DCB ($m = n = 1$, $\Delta a/t = 0.125$)

t/T	1.0	0.8	0.6	0.4	0.2
K_{II}/K_I (present)	0.0	0.192	0.433	0.742	1.15
K_{II}/K_I (2D)	0.0	0.153	0.333	0.530	0.705
G/G_t	1.008	1.008	0.992	0.995	0.992

Table 2
Convergence with increasing sublamine ($t/T = 0.5$, $\Delta a/t = 0.125$)

$m-n$	1-1	1-2	2-4	4-8	2D
K_{II}/K_I	0.560	0.526	0.435	0.433	0.431

Table 3
Converged results for different thickness ratios of a DCB ($\Delta a/t = 0.125$)

t/T	1.0	0.8	0.6	0.4	0.2
$m-n$	1-1	2-3	2-4	2-5	2-8
K_{II}/K_I (present)	0.0	0.154	0.325	0.537	0.730
K_{II}/K_I (2D)	0.0	0.153	0.333	0.530	0.705

7. Avoidance of oscillatory behaviour of energy release rates

Raju et al. (1988) investigated the convergence of energy release rate components for edge delamination at the $-35^\circ/90^\circ$ interface of an eight-ply $[0^\circ/\pm 35^\circ/90^\circ]_s$ composite laminate subjected to uniform axial tensile strain, as shown in Fig. 6, using quasi-three-dimensional (Q3D) finite element analysis in conjunction with VCCT. Two models were adopted. One was a ‘bare’ interface laminate, i.e. a conventional laminate without resin-rich layers. The energy release rate components exhibit oscillatory behaviour. In the second model, a ‘resin’ interface layer was introduced, within which the delamination is embedded. The ‘resin’ layer has a thickness of 0.01 mm between the $-35^\circ/90^\circ$ plies. With the delamination located in a homogeneous isotropic material, the oscillatory components in the expressions for the energy release rates vanish.

The ‘bare’ interface laminate is re-analysed using the present approach. Due to the symmetry, only one quarter of the laminate is analysed. This is divided into a number of sublaminates as indicated in Table 4.

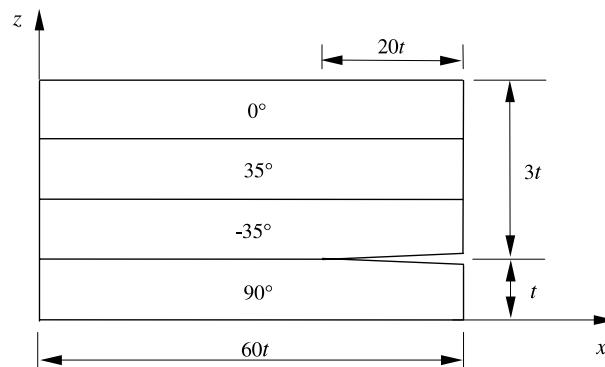
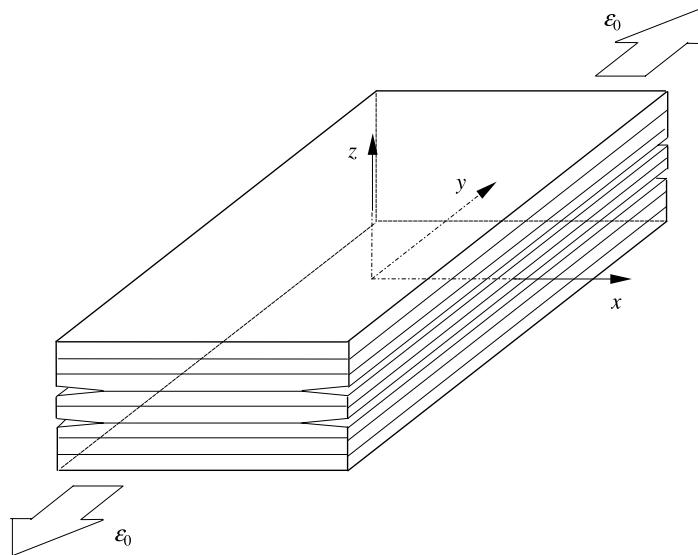
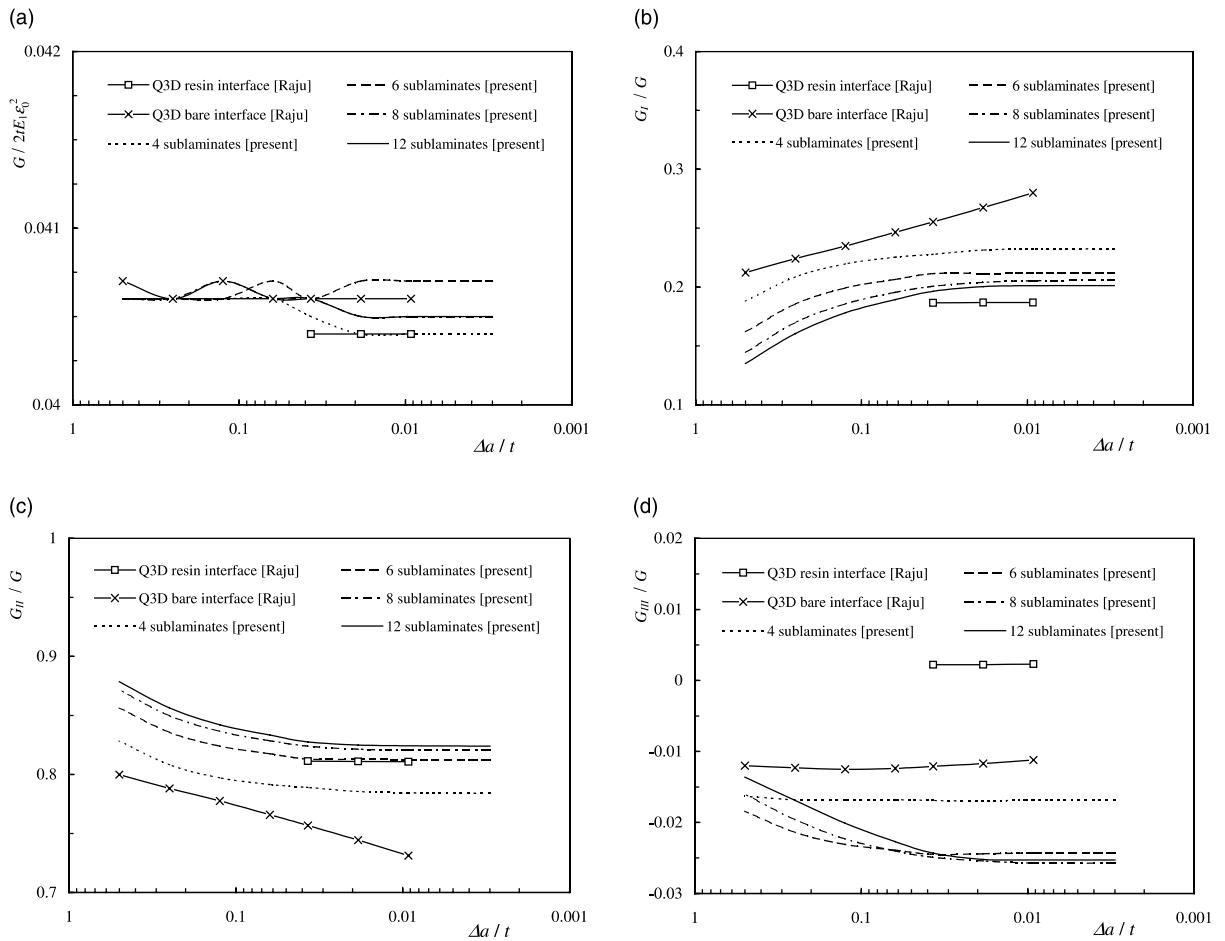


Fig. 6. Edge delamination in $[0^\circ / \pm 35^\circ / 90^\circ]_s$ laminate (fibre orientation is with respect to y axis).

Table 4

Number of sublaminates and their thicknesses in plies of $[0^\circ/\pm 35^\circ/90^\circ]$ laminate

Sublaminates	0°	35°	-35°	90°
4	t	t	t	
6	t	t	$t/2$	$t/2$
8	t	t	$t/2$	$t/4$
12	$t/2$	$t/2$	$t/2$	$t/8$
			$t/2$	$t/8$
			$t/4$	$t/4$
			$t/8$	$t/8$
			$t/4$	$t/4$
				$t/2$

Fig. 7. Total energy release rate and percentage of individual modes of edge delamination under uniaxial tension (E_1 is the longitudinal Young's modulus).

The size Δa of the delamination tip element is made smaller and smaller in order to show the convergence of the energy release rates in the same way as did Raju et al. (1988). The present numerical results together with those of Raju et al. are shown in Fig. 7.

The Q3D results for the 'bare' interface model given by Raju et al. (1988) show that the total energy release rate remains unchanged as the size of the delamination tip element decreases over the range given in Fig. 7. In fact, all the models agree on this, and the differences are negligible, given the scale of the vertical

axis of the graph. However, the non-convergence behaviour for the individual modes from Q3D with the 'bare' interface is clear, although the oscillation is not yet apparent. To exhibit this, one requires a very small Δa which is usually too small for a practical finite element mesh. Analytical expressions for the oscillatory terms can be found in Sun and Jih (1987) and Raju et al. (1988). The individual energy release rates converge for all given values of $\Delta a/t$ when the resin interface model is used. Compared with the results for the 'resin' interface model, Raju et al. (1988) found that the range of Δa from 0.5 to 0.25 of the ply thickness t gives similar results to those of the 'bare' interface model. However, without an extensive parametric study, this may not be so in other cases.

The results for the present sublaminates model show that the total energy release rate and its individual components converge as the size of the delamination tip element decreases, showing the same trend as that of the Q3D 'resin' interface model. Furthermore, the converged values agree well with the 'resin' interface model. Even when a coarse mesh of, say, four sublaminates (one ply, one sublaminates) is used, the approximation obtained is acceptable for most engineering applications.

Fig. 8 shows the distributions of the stress resultants and moments in the part of the laminate above the delamination. As expected, the tension, in-plane shear and transverse shear forces are continuous on both

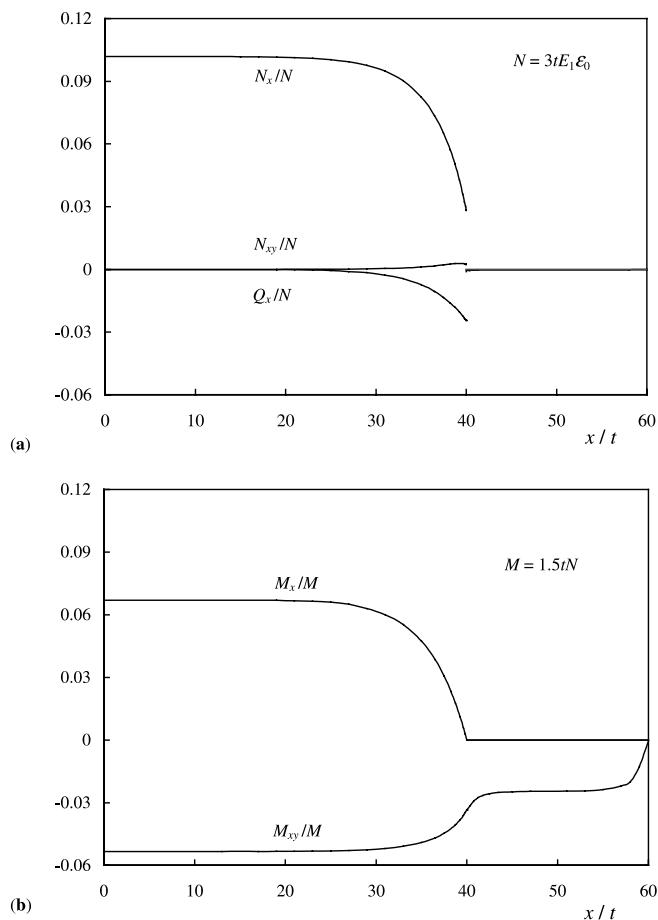


Fig. 8. Distribution of stress resultants and moments above the edge delamination plane (moments are calculated with respect to the delamination plane).

sides of the delamination tip, but discontinuities, i.e. concentrated interfacial forces F_x , F_y and F_z , are found at the delamination tip, the moments calculated with respect to the delamination plane are continuous along the whole region and no jumps occur across the delamination tip.

Obviously, F_y is much smaller than F_x and F_z and, as a result, G_{III} is much smaller than G_I and G_{II} , see Fig. 7. However, although F_z and F_x are of similar magnitudes, the mode I energy release rate may be rather different from that of mode II, because energy release rates are also associated with the relative opening and sliding displacements which depend on the bending, shear and tension stiffnesses of the sublaminates. There may be large differences between these relative displacements.

Due to the existence of delamination, the stress resultants change dramatically across the delamination tip. The coupling effects between tension and shear make the relative sliding and tearing (modes II and III) displacement of the delamination depend upon both interlaminar shear stress components ahead of the delamination tip. This means that the nodal force and the corresponding displacement of the minor of the coupled modes II and III can be in opposite directions. As a result, the energy release rate of the corresponding mode becomes negative, as with G_{III} in the present case. A similar phenomenon can be found in a biaxial stress state. The minor stress components may do negative work on the corresponding strain as a result of Poisson's ratio effects. In the resin interface layer model used by Raju et al. (1988), mode II and mode III components of the energy release rate are both positive because there does not exist such tension-shear coupling in the isotropic resin layer.

8. Conclusions

By modelling the laminate as an assembly of sublaminates, the evaluation of the total energy release rate and its individual components for delaminations in composite laminates have been achieved using the virtual crack closure technique. The stress resultant jumps across the delamination tip in the laminate theory help to avoid the singularity along with the oscillatory behaviour around the delamination tip encountered in conventional fracture mechanics. The individual as well as the total energy release rates, therefore, converge to definite values as the mesh around the delamination tip is refined in the present approach. The use of sublaminates helps to reduce the size of the problem in the thickness direction to an extent.

The numerical results for DCB and edge delamination in a composite laminate show good agreement with those obtained from other methods in the literature. Compared with the solid finite element method with a resin interface, the present approach requires far fewer elements (sublaminates) through the laminate thickness. The accuracy can be controlled by adjusting the number of sublaminates in the laminate. Even with a small number of sublaminates, reasonable approximations can be obtained. It is, therefore, an effective approach for analysing delaminated laminates and for obtaining energy release rates so that the propagation of a delamination can be predicted using an appropriate criterion.

When a delaminated laminate under a generalised plane strain state, as analysed in the present paper, is considered as a segment perpendicular to the front of a delamination of a general shape in a laminate, the approach can be extended to deal with delaminations of arbitrary shape. Moreover, this approach is simple and can be implemented in most commercial finite element codes in a straightforward manner.

References

- Anderson, T.L., 1995. Fracture Mechanics. Second edition, CRC Press, Boca Raton, FL.
- England, A.H., 1965. A crack between dissimilar media. *J. Appl. Mech.* 32, 400–402.
- HKS, 1996. ABAQUS. Version 5.6.

- Hutchinson, J.W., Suo, Z., 1992. Mixed mode cracking in layered materials. In: Advances in Applied Mechanics, Vol. 28, Academic Press, New York.
- Hwu, C., Hu, J.S., 1992. Stress intensity factors and energy release rates of delaminations in composite laminates. *Engng. Fract. Mech.* 42, 977–988.
- Raju, I.S., Crews Jr., J.H., Aminpour, M.A., 1988. Convergence of strain energy release rate components for edge-delaminated composite laminates. *Engng. Fract. Mech.* 30, 383–396.
- Reissner, E., 1945. The effect of transverse shear deformation on the bending of elastic plate. *J. Appl. Mech.* 12, 69–76.
- Rice, J.R., 1988. Elastic fracture mechanics concepts for interfacial cracks. *J. Appl. Mech.* 55, 98–103.
- Rice, J.R., Sih, G.C., 1965. Plane problems of cracks in dissimilar media. *J. Appl. Mech.* 32, 418–423.
- Rybicki, E.F., Kanninen, M.F., 1977. A finite element calculation of stress intensity factors by a modified crack closure integral. *Engng. Fract. Mech.* 9, 931–938.
- Sheinman, I., Kardomateas, G.A., 1997. Energy release rate and stress intensity factors for delaminated composite laminates. *Int. J. Solids Struct.* 34, 451–459.
- Sun, C.T., Jih, C.J., 1987. On strain energy release rates for interfacial cracks in bi-material media. *Engng. Fract. Mech.* 28, 13–20.
- Suo, Z., 1990. Singularities, interfaces and cracks in dissimilar anisotropic media. *Proc. R. Soc. Lond.* A427, 331–358.
- Suo, Z., Hutchinson, J.W., 1990. Interface crack between two elastic layers. *Int. J. Fract.* 43, 1–18.
- Toya, M., Aritomi, M., Chosa, A., 1997. Energy release rates for an interface crack embedded in a laminated beam subjected to three-point bending. *J. Appl. Mech.* 64, 375–382.
- Wang, S.S., 1983. Fracture mechanics for delamination problems in composite materials. *J. Compos. Mater.* 17, 210–223.
- Williams, M.L., 1959. The stress around a fault or crack in dissimilar media. *Bull. Seismol. Soc. Am.* 49, 199–204.
- Williams, J.G., 1988. On the calculation of energy release rates for cracked laminates. *Int. J. Fracture* 36, 101–119.
- Wu, K.C., 1990. Stress intensity factors and energy release rate for interfacial cracks between dissimilar anisotropic materials. *J. Appl. Mech.* 57, 882–886.